Supporting Information

Integrating Prussian Blue Analog-based Nanozyme and Online Visible Light Absorption Approach for Continuous Hydrogen Sulfide Monitoring in Brains of Living Rat

Chao Wang, Manchao Wang, Wang Zhang, Jia Liu, Mingju Lu, Kai Li, Yuqing Lin*

Department of Chemistry, Capital Normal University, 105 West Third Ring Road North, Haidian District, Beijing, 100048, China

*Corresponding author: Y. Lin.

Tel.: +861068903047; Fax: +861068903047; E-mail address: linyuqing@cnu.edu.cn.

Contents

EXPERIMENTAL SECTION

Reagents. Nickel nitrate hexahydrate ($Ni(NO_3)_2 \cdot 6H_2O$), potassium hexacyanoferrate(III) ($K_3[Fe(CN)_6]$), trisodium citrate dihydrate, 3,3',5,5'-tetramethylbenzidine (TMB), nicotinamide adenine dinucleotide (NADH), 1,2-diaminobenzene (OPD), sodium sulfide (Na_2S), dopamine (DA), 3,4-dihydroxyphenylacetic acid (DOPAC), ascorbic acid (AA), glutamate (Glu), glycine (Gly), uric acid (UA), hydrogen peroxide (H_2O_2), glutathione (GSH), glutathione disulfide (GSSG), cysteine (Cys), histidine (His) and glucose were all purchased from Sigma (Shanghai, China). Other chemicals were purchased from Beijing Chemical Reagent Company (Beijing, China). All reagents were of analytical reagent grade and used as received. The aqueous solutions were prepared with deionized (DI) water produced by a Milli-Q system (Millipore, Bedford, MA, USA, 18.2 MΩ•cm). The artificial cerebrospinal fluid (aCSF) (126 mM NaCl, 2.4 mM KCl, 1.1 mM $CaCl_2$, 0.85 mM $MgCl_2$, 27.5 mM $NaHCO_3$, 0.5 mM Na_2SO_4, 0.5 mM KH_2PO_4, pH 7.4) was used as the solution for H_2S detection.

Instrumentation. All images of the solutions inside the capillary (Φ250 μm) were captured in bright field mode, and the following real-time light intensity conversions were accomplished by an inverted fluorescence microscope (IX73, Olympus, USA) equipped with CellSens Dimension 2.1 software. To characterize the morphology and chemical structure of as-synthesized Prussian blue analog nanocubes (PBA NCs), SEM (Scanning Electron Microscopy) images were obtained using a Hitachi S-2600N scanning electron microscope. TEM (Transmission Electron Microscope) images, HRTEM (High-Resolution Transmission Electron Microscopy),

elemental mapping and EDS (Energy-Dispersive Spectroscopy) analyses were performed on a JEM-2100F transmission electron microscope operated at 200 kV. FTIR (Fourier-Transform Infrared) spectra were collected with a Bruker Equinox55 spectrophotometer; Raman spectra were collected with a Renishaw inVia Reflex Raman microscope; XRD (X-ray Powder Diffraction) was carried out on a Bruker D8 advance powder diffractometer with Cu Ka radiation; XPS (X-ray Photoelectron Spectra) measurements were performed on an ESCA Lab 250 X-ray photoelectron spectrometer using a monochromatic Al Ka radiation excitation source. The UV-visible absorption spectra were obtained by using a 1 cm path length quartz cell at room temperature using a Shimadzu UV-2550 UV-vis spectrophotometer.

Synthesis of PBA NCs. Prussian blue analog nanocubes (PBA NCs) were prepared following a reported method.[S1] In a typical synthesis, 0.9 mmol of trisodium citrate dihydrate and 0.6 mmol of $Ni(NO_3)_2 \cdot 6H_2O$ were dissolved in 20 mL of distilled water as solution A, while 0.4 mmol of $K_3[Fe(CN)_6]$ was dissolved in 10 mL of distilled water as solution B. Then, solution B was quickly added into solution A at room temperature under vigorous magnetic stirring for 1 min. Then, the beaker was sealed and heated at 40 °C for 24 h. Next, the precipitate was collected by centrifugation, washed twice with doubly distilled water, and then dried at 60 °C overnight.

Analysis of Oxidase-like Activity. In this section, three kinds of substances (TMB, OPD and NADH) were chosen to verify the oxidase-like activity of the PBA NCs. The reaction solution (2 mL, pH 7.0) containing each substance (1 mL, 2 mM) and PBA NCs (1 mL, 100 μg/mL) was mixed at room temperature. Then, the mixed

solutions were investigated by measuring the UV-vis absorbance on the spectrophotometer.

In Vivo Microdialysis and H_2S Monitoring in a Living Brain. Surgeries for in vivo microdialysis were performed following previously reported methods.[S2] Briefly, adult male Sprague-Dawley rats (SD rats, weighing 300 ± 50 g) were obtained from Vital River Laboratory Animal Technology Co., Ltd. (Beijing, China). The rats were housed individually with a 12:12 h light/dark schedule and with food and water available ad libitum. Briefly, guide tubes were inserted into rats, and the rats were anesthetized by chloral hydrate (350 mg/kg i.p.). Throughout the surgery, the body temperature of the rats was maintained at 37 °C with a heating pad. After the surgery, the rats were individually placed into a warm incubator until they recovered from anesthesia. The rats were allowed to recover for a day before microdialysis and online optical detection. For the global cerebral ischemia model, the microdialysis probe (2 mm in length; Bioanalytical Systems Inc. (BAS), BAS Carnegie Medicine) was implanted into the brain cortex region (AP=0.6 mm, L=2.8 mm from bregma, V=1 mm from the surface of the skull) according to standard stereotaxic procedure.[S3] The microdialysis sampling was perfused with aCSF at a flow rate of 2 μL/min to monitor the cerebral H_2S levels, and the microdialysates were introduced into the OODP for continuous measurements. The surgical procedures for two-vessel occlusion (2-VO) ischemia were undertaken during the period of in vivo microdialysis and on-line optical measurements. The global ischemia model was constructed with occlusion of the bilateral common carotids arteries with nontraumatic arterial clips. For the

awake/anesthetized model and the Na_2S intraperitoneal injection model, the microdialysis probe (4 mm in length; Bioanalytical Systems Inc. (BAS), BAS Carnegie Medicine) was implanted into the brain hippocampal region (AP=4.5 mm, L=4.2 mm from bregma, V=2.5 mm from the surface of the skull) according to standard stereotaxic procedures.[S4] The microdialysis sampling was perfused with aCSF at a flow rate of 2 μL/min to monitor the cerebral H_2S levels, and the microdialysates were introduced into the OODP for continuous measurements. The awake/anesthetized state was accomplished by controlling the volume of chloral hydrate (350 mg/kg i.p.). Another model was performed following a previously reported method.[S5] The 0.9 % saline (0.1 mL) and Na_2S solution (0.1 mL, 40.8 mg/kg) were injected into the same rat by intraperitoneal injection. During all the surgeries, the body temperatures of the rats was maintained at 37 °C with a heating pad. All efforts were made to reduce both animal suffering and the number of animals used.

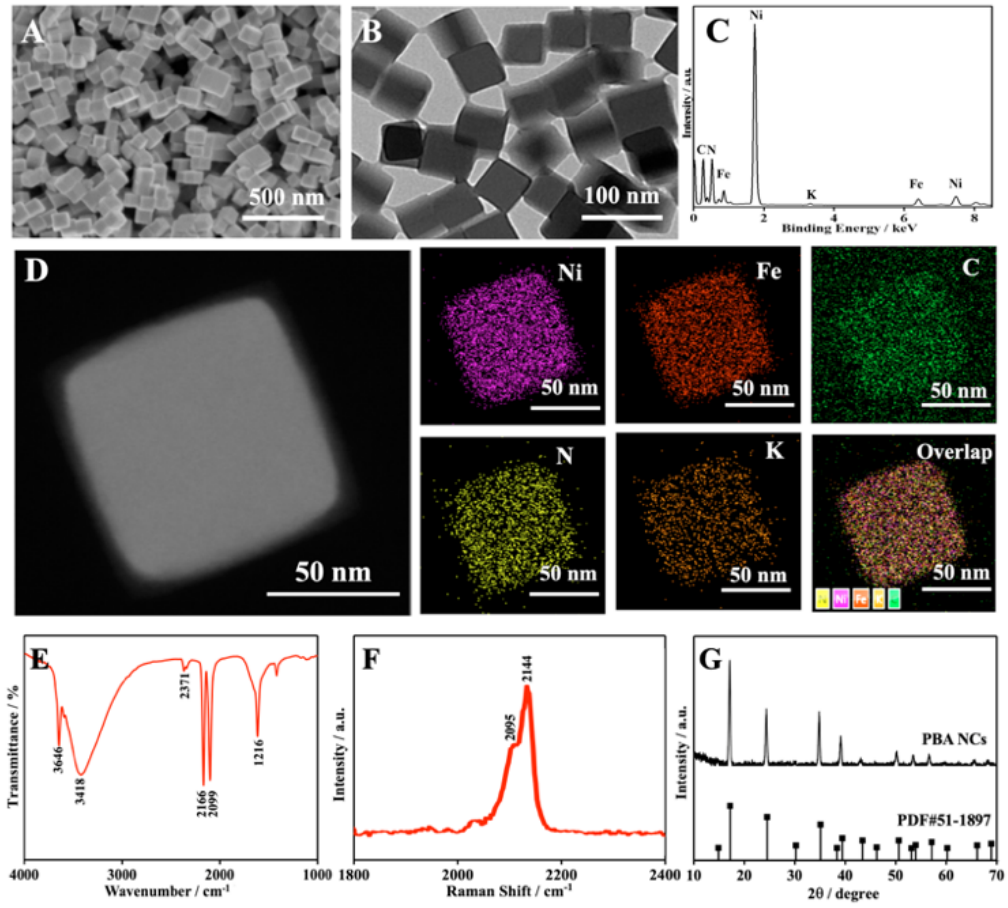

Figure S1. Typical SEM images (A), TEM images (B), EDS spectra (C), element mapping images (D), FT-IR spectra (E), Raman spectra (F) and XRD spectra of PBA NCs.

A high-performance enzyme-mimicking nanozyme was designed for H_2S monitoring. Nickel iron bimetal Prussian blue analog nanocubes (PBA NCs) were prepared through 40 ℃ water bath-assisted synthesis for mimicking oxidase-like activity. Based on the SEM and TEM images (Figure S1A and B), the PBA NCs exhibited cubic morphology, smooth surfaces, and an average size of 60 nm. The main bimetal elements of Ni and Fe, as well as C, N and K were present and uniformly distributed in PBA NCs, as illustrated in the EDS spectra (Figure S1C) and elemental mapping images (Figure S1D). To further characterize the chemical structure of the nanocubes, FT-IR, Raman, XRD and XPS spectra of the PBA NCs were

measured. The typical characteristic peaks at 2166 cm^{-1} and 2099 cm^{-1} in the FT-IR spectra (Figure 1E), as well as the peaks at 2144 cm^{-1} and 2095 cm^{-1} in the Raman spectra, corresponded to the Fe^{III}-CN-Ni^{II} and Fe^{II}-CN-Ni^{II} vibration modes of the CN group, respectively.[S7] Other peaks in FT-IR were attributed to the CO_2 and H_2O of the air. The diffraction pattern of PBA NCs are in good agreement with the standard patterns of JCPDS No. 51-1897 (Figure 1G), which indicated that the main compound of PBA NCs were $KNi[Fe(CN)_6]$. Those characteristic peaks at 17.30º, 24.57º, 35.02º and 39.31º correspond to the (200), (220), (400) and (420) planes of $KNi[Fe(CN)_6]$, respectively.[S1]

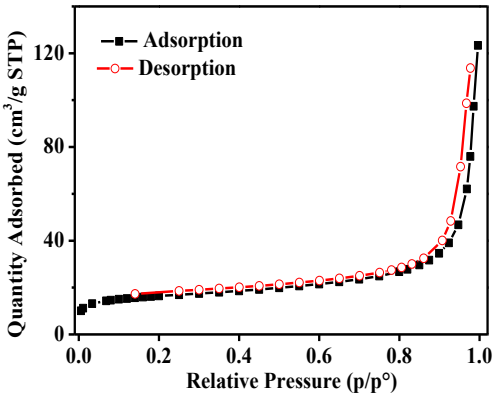

Figure S2. N_2 adsorption isotherm of the PBA NCs.

The specific surface area of 60.12 m^2/g was measured by nitrogen adsorption and calculated using the Barrett-Joyner-Halenda (BJH) model (Figure S2). Compared with previous reports, the small PBA NCs have a larger specific surface area, which may be attributed to the water bath-assisted synthesis process.[S1] In addition, more catalytic active sites for the enzyme mimicking reaction were present.

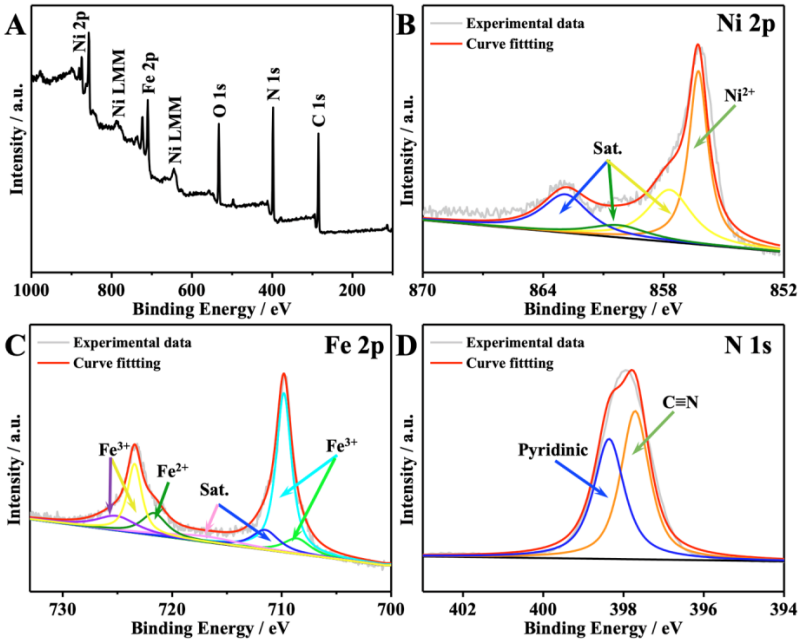

Figure S3. (A) XPS survey spectra of PBA NCs, and (B-D) high-resolution XPS spectra of Ni 2p, Fe 2p and N 1s.

XPS spectra were collected to investigate the surface chemical compositions and valence states of the PBA NCs. As shown in Figure S3A, Ni, Fe, C and N elements were presented in the overall XPS spectra of PBA NCs. In the high-resolution XPS spectra of Ni 2p spectra (Figure S3B), the peak at 856.3 eV was attributed to Ni^{2+}, and peaks at 857.7 eV, 860.2 eV and 862.9 eV were belonged to its satellite peaks.[S8] In Fe 2p spectra (Figure S3C), Fe^{3+} (708.6 eV, 709.8 eV, 723.4 eV, 725.1 eV) and Fe^{2+} (721.6 eV) were mainly forms of iron in PBA NCs.[S1] In N 1s spectra (Figure S3D), C≡N bond (397.1 eV) and pyridinic-N (398.4 eV) existed in PBA NCs.[S9] Those results also agreed with $KNi[Fe(CN)_6]$ in the XRD results.

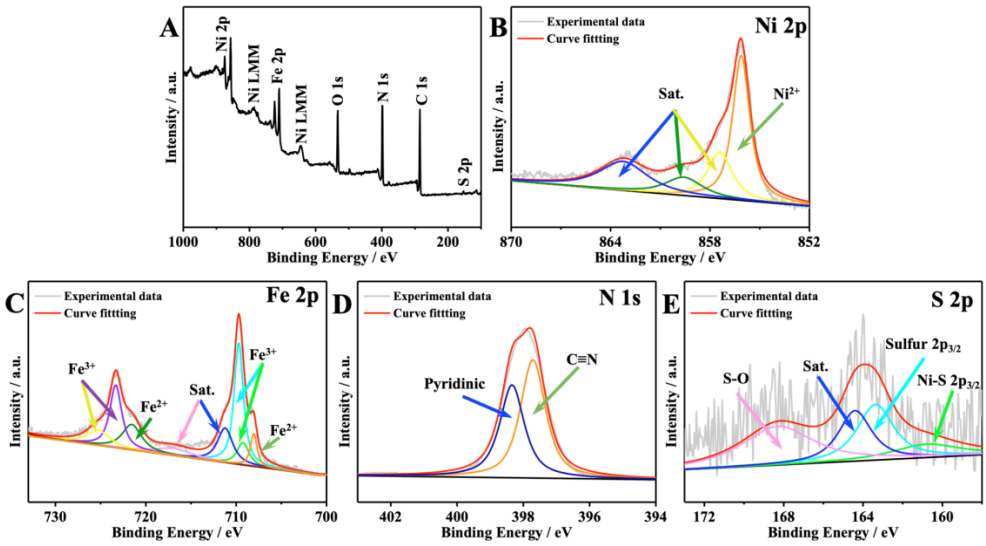

Figure S4. (A) XPS survey spectra of PBA NCs after H_2S addition, and (B-E) high-resolution XPS spectra of Ni 2p, Fe 2p, N 1s and S 2p.

Firstly, the Ni, Fe, C, N and S elements presented in the overall XPS spectra of PBA NCs after H_2S addition (Figure S4A). Then, in the high-resolution XPS spectra of Ni 2p spectra (Figure S4B), the peak at 856.1 eV was attributed to Ni^{2+}, and peaks at 857.4 eV, 859.6 eV and 863.2 eV were belonged to its satellite peaks.[S8] In Fe 2p spectra (Figure S4C), Fe^{3+} (709.2 eV, 709.7 eV, 723.3 eV, 725.2 eV) and Fe^{2+} (708.1 eV, 721.5 eV) existed.[S1] In N 1s spectra (Figure S4D), C≡N bond (397.7 eV) and pyridinic-N (398.3 eV) appeared.[S9] Furthermore, the S 2p spectra (Figure S4E) suggested that binding energy located at 160.8 eV can be corresponded to S $2p_{3/2}$ in Ni-S bond, while another peak at 163.4 eV was attributed to S $2p_{3/2}$ in sulfur elementary state.[S10] The peaks at 164.4 eV and 168.3 eV were belonged to satellite peak of S $2p_{3/2}$ and S-O bond, respectively.[S11]

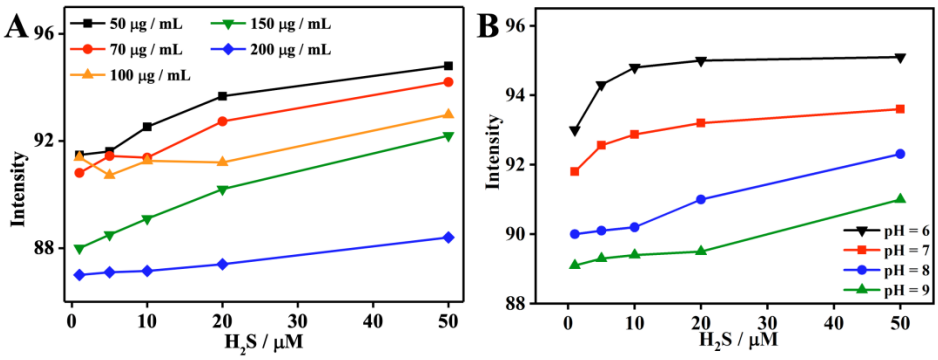

Figure S5. (A) The light intensity of H_2S against mixed with different concentration of PBA NCs. (B) The light intensity of PBA NCs (150 μg/mL) added with H_2S under different pH. The concentrations of H_2S were 1, 5, 10, 20 and 50 μM.

Table S1. Comparison of the present method with other approaches for H_2S online measurement.

Methods	Online electrochemical system	Online droplet-based microfluidic fluorescent system	Online optical detection platform
Microfluidic chip	Yes	Yes	No
Sensors	$[Ru(NH_3)_6]^{3+}$/ ITO electrode	AuNP–GSH-FITC probe	PBA NCs/TMB system
Mechanisms	$[Ru(NH_3)_6]^{3+}$ catalyze the electrochemical oxidation of H_2S	Legends exchange between H_2S and GSH on AuNP	PBA NCs etched by H_2S and oxidase-like activity decreased
Detecting Signals	Current	Fluorescence	Light intensity
Real-time detection	Real-time	Non-real time	Real-time
Linearity	0.5-10 μM	5.0-50 μM	0.1-20 μM
LOD	0.17 μM	2.0 μM	0.033 μM
Ref.	[S5]	[S4, S6]	This work

REFERENCES

(S1) Zou, H. H.; Yuan,C. Z.; Zou, H. Y.; Cheang, T. Y.; Zhao, S. J.; Qazi, U. Y.; Zhong, S. L.; Wang, L.; Xu, A. W. *Catal. Sci. Technol.* **2017**, *7*, 1549-1555.

(S2) Lin, Y. Q.; Lu, X. L.; Gao, X.; Cheng, H. J.; Ohsaka, T.; Mao, L. Q. *Electroanal.* **2013**, *25*, 1010-1016.

(S3) Liu, K.; Yu, P.; Lin, Y. Q.; Wang, Y. X.; Ohsaka, T.; Mao, L. Q. *Anal. Chem.* **2013**, *85*, 9947-9954.

(S4) Gu, F. D.; Zhou, X. Y.; Zhu, X. C.; Zhao, M. P.; Hao, J.; Yu, P.; Mao, L. Q. *Analyst* **2015**, *140*, 3814-3819.

(S5) Wang, S. J.; Liu, X. M.; Zhang, M. N. *Anal. Chem*. **2017**, *89*, 5382-5388.

(S6) Zhu, X. C.; Xu, L.; Wu, T. B.; Xu, A. Q.; Zhao, M. Q.; Liu, S. R. *Biosens. Bioelectron.* **2014**, *55*, 438-445.

(S7) Ren, W. H.; Qin, M. S.; Zhu, Z. X.; Yan, M. Y.; Li, Q.; Zhang, L.; Liu, D. N.; Mai, L. Q. *Nano. Lett.* **2017**, *17*, 4713-4718.

(S8) Yu, X. Y.; Feng, Y.; Jeon, Y.; Guan, B.; Lou, X. W.; Paik, U. *Adv. Mater.* **2016**, *28*, 9006-9011.

(S9) Cao, Z. K.; Duan, A. J.; Zhao, Z.; Li, J. M.; Wei, Y. C.; Jiang, G. Y.; Liu, J. *J. Mater. Chem. A* **2014**, *2*, 19738-19749.

(S10) Liang, H.; Gandi, A. N.; Anjum, D. H.; Wang, X.; Schwingenschlögl, U.; Alshareef, H. N. *Nano Lett.* **2016**, *16*, 7718-7725.

(S11) Ahn, W.; Park, M. G.; Lee, D. U.; Seo, M. H.; Jiang, G. P.; Cano, Z. P.; Hassan, F. M.; Chen, Z. W. *Adv. Funct. Mater.* **2018**, *28*, 1802129.